GEOLOGICAL MAP OF THE HUMBOLDTIANUM BASIN AND ITS DEPOSITS. E. F. Schmidt[1] and P. D. Spudis[2], [1]Department of Physics, Embry-Riddle Aeronautical University, 3700 Willow Creek Rd., Prescott, AZ 86301 (schmide2@my.erau.edu), [2]Lunar and Planetary Institute, 3600 Bay Area Blvd., Houston, TX 77058

Introduction: Humboldtianum basin is a Nectarian-age multi-ring basin centered at approximately 57º N, 82º E. The inner ring is roughly 275 km in diameter and the outer ring is estimated at around 650 km in diameter [1]. Although the basin was previously studied and mapped [2], new image data from Lunar Reconnaissance Orbiter (LRO) and chemical and mineral concentration data from Clementine and Lunar Prospector provide improved surface image resolution and information on the composition of basin deposits, allowing updated and improved maps to be compiled and new inferences made on the composition of basin ejecta and its crustal target.

The basin is asymmetric and morphologically complex. The area to the south and west of the basin is similar to other lunar basins but the area to the north and east does not have a well-defined outer ring. Bel'kovich crater appears to overlie Humboldiatum's inner ring in this area. The unusual shape of the basin may indicate its formation from an oblique impact, as has been proposed for some other basins [3].

The purpose of this project was to create a geological map centered on the Humboldtianum basin, allowing a better understanding of the composition of its ejecta deposits and crustal target. In addition, due to its age, compositional analysis was used to help determine the level of influence of the younger Imbrium and Crisium ejecta on Humboldtianum itself. This was done by mapping all the important units related to the basin, which included their relative ages, and looking for compositional clues as to their origin. The image data for this map came from narrow-angle and wide-angle Lunar Reconnaissance Orbiter Cameras (LROC), the LRO GLD-100 topographic map [4], along with data on TiO_2 and FeO content from Clementine images [5] and thorium concentration data from Lunar Prospector [6]. This map can be used to help future lunar mission planning and in determining the basin target composition. In addition, this new map may help develop a better understanding of how Bel'kovich and Humboldtianum are related.

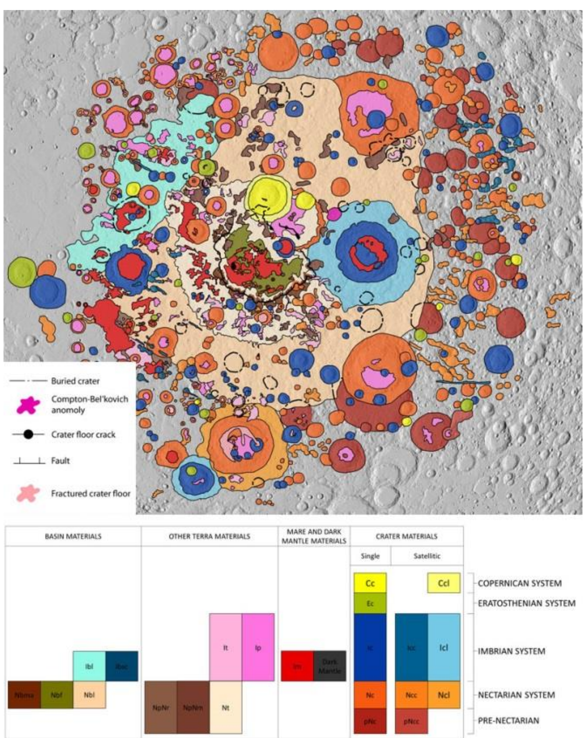

Figure 1 – New geological map of the Humboldtianum basin.

Methods: Basin-centered orthographically projected LRO images and topographic maps were used in ArcGIS 10.1 to assist in the determination and mapping of the different stratigraphic units around the basin based on relative age, elevation changes, surface texture, albedo, FeO content (to help distinguish between plains and mare), and position. To improve comparisons and provide continuity with existing maps, mapping conventions were based on those used in the 1978 USGS map of the lunar north side [2]. Only craters of greater than 20 km in diameter were included in the map allowing the focus to remain on the basin-related units.

After the new map was finished, compositional maps were overlaid onto it, allowing for the concentrations of Fe, Ti, and Th to be determined for each geological unit and region of the basin and its surrounding area.

Results: A total of 23 geological units were mapped (Fig. 1). The units were divided into four categories: basin materials, other terra materials, mare and dark mantle material, and crater deposits. Mapped units ranged from pre-Nectarian to Copernican.

In addition, important non-stratigraphic geologic features were mapped, including large cracks in the Bel'kovich floor, the fault indicating the outer edge of the basin, the Compton-Bel'kovich thorium anomaly, and craters buried by basin and other crater ejecta.

The results of the chemical composition data are shown in Figure 2 and Table 1 below. Figure 2 shows the concentration of Fe, Ti, and Th by region around the basin. Table 1 contains the chemical concentrations of the units around the basin.

Analysis: Based on the data from Figure 2, although the uncertainties are large, a general negative gradient in FeO content can be seen from the north-west to the south-east, where the region mapped as Imbrium ejecta is the highest in Fe (most mafic). This indicates a slightly larger influence from Imbrium than is detectable from the mapping in Figure 1. However, due to the formation of subsequent large craters and mare flooding in the area, it is difficult to determine if this high FeO wt % is due solely to Imbrium ejecta or if there is some other cause.

Although there is also a general negative trend in thorium concentrations heading east, a spike can be seen in the Compton ejecta and in the Bel'kovich region. This is caused by the Compton-Bel'kovich thorium anomaly, marked in Figure 1, which has a very high thorium content relative to the rest of the basin region (see Table 1). This feature has been proposed as the site of the eruption of silicic volcanic rocks (i.e. rhyolite), a very rare phenomenon on the Moon [7].

Other than the high concentrations of FeO in the dark mantle and mare, the other units are all of feldspathic highlands composition, with little variation. Compared with the composition of the other basins previously studied [8-11], Humboldtianum ejecta is low in FeO, even lower than Orientale, which is very iron-poor (Fig. 3). This result suggests that the ejecta from Humboldtianum is extremely feldspathic and the basin crustal target likely consisted of very ancient anorthositic rocks, which appear common in the northern central far side highlands [12].

The TiO_2 content of the ejecta is fairly uniform throughout the region with the two notable exceptions of Compton-Bel'kovich and the terra material (Nt) inside Bel'kovich. The low concentration of TiO_2 inside Bel'kovich could be related to the influence of the thorium anomaly approximately 100 km away.

The average elevation south of the basin is much higher than the average elevation north of it such that the peaks of the northern massifs are approximately equal in elevation as the southern highlands. Moreover, many massifs exist in the northern areas but not in the southern. One possible explanation for this relation is that the basin-forming impact hit at an oblique angle pointing in a northerly direction. It should be noted that the highest elevation in the south is approximately the same as the peaks of the massifs in the north.

Compared with other recently mapped basins, Imbrium, Orientale, and Crisium [9-11], Humboldtianum contains lower levels of Ti and, on average, lower levels of Fe. Notably, impact melts were not found during the mapping process. This is either because they do not exist or they do exist but are now covered by younger impact materials.

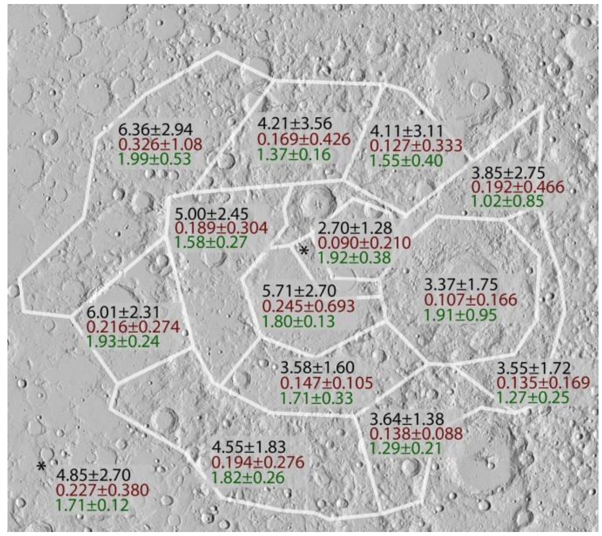

Figure 2 – Regional mineral weight %. Black: FeO, Red: TiO_2, Green: Thorium (ppm). Uncertainties indicate ± 1σ

Conclusions: A new geological map of the Humboldtianum basin was created using new data from the LRO, Clementine, and Lunar Prospector missions. The chemical data was overlaid onto the geographic map and related to mapped ejecta units around the basin, and stratigraphic units were recorded and analyzed.

The compositional analysis shows that the different units had similar mineral content. However, there was a noticeable difference in FeO content in the different regions of the basin, a negative content gradient was found to exist from the north-west to the south-east. This indicates that there is a large Imbrium influence on that side of the basin but much less, if any, influence on the side of Humboldtianum basin away from Imbrium.

It was also found that large massifs are found north of the basin while the region to the south is more uniform in elevation, with fewer massifs present in the area.

References: [1] Wilhelms, D. E. (1987) *The Geologic History of the Moon*. USGS Prof. Paper 1348, 302 pp. [2] Lucchitta, B. K. USGS map I-1062. [3] Schultz, P. H., Crawford, D. A. (2016) doi:10.1038/nature18278 [4] Scholten, F. et al. (2012) doi:10.1029/2011je003926 [5] Lucey P.G. et al. (2000) JGR 105, 20297. [6] Lawrence D. et al. (2007) GRL 34, L03201, doi:10.1029/2006GL028530. [7] Jolliff, B. L. et al. (2011) LPSC. [8] Smith, M. C., Spudis, P. D. (2013) LPSC. [9] Martin, D. J. P., Spudis, P. D. (2014) LPSC [10] Murl, J. N., Spudis, P. D. (2015) LPSC [11] Sliz, M. U., Spudis, P. D. (2016) LPSC. [12] Jolliff, B. L. et al. (2000) JGR 105, 4197.